

3-2010

Kinetics of SO₂ Absorption with Fly Ash Slurry with Concomitant Production of a Useful Wastewater Coagulant

Ling Li
Iowa State University

Maohong Fan
Georgia Institute of Technology

Robert C. Brown
Iowa State University, rcbrown3@iastate.edu

Jacek A. Koziel
Iowa State University, koziel@iastate.edu

Johannes van Leeuwen
Follow this and additional works at: https://lib.dr.iastate.edu/abe_eng_pubs
Iowa State University, leeuwen@iastate.edu

 Part of the [Bioresource and Agricultural Engineering Commons](#), [Environmental Engineering Commons](#), and the [Environmental Sciences Commons](#)

The complete bibliographic information for this item can be found at https://lib.dr.iastate.edu/abe_eng_pubs/906. For information on how to cite this item, please visit <http://lib.dr.iastate.edu/howtocite.html>.

Kinetics of SO₂ Absorption with Fly Ash Slurry with Concomitant Production of a Useful Wastewater Coagulant

Abstract

This research was aimed at recovering Fe and Al compounds to produce a useful complex coagulant from fly ash using H₂SO₄ and SO₂ from flue gas oxidized to SO₃ by NaClO₃. The reaction kinetics of wet SO₂ scrubbing from simulated flue gas with fly ash slurry was studied. The SO₂ scrubbing experiments were carried out in a jacketed glass reactor system with a simulated flue gas containing SO₂ and N₂ in the gas phase and fly ash slurry in the liquid phase. Sodium chlorate was added to oxidize SO₂ to SO₃, adding H₂SO₄ in the slurry. The reaction orders of both Fe₂O₃ and Al₂O₃ extraction from fly ash slurry were shown to be 1.5. The empirical Arrhenius expressions were also derived from the reaction rate constants obtained at each reaction temperature. The mass transfer process of SO₂ with ClO₃⁻ was evaluated using a two-film theory model.

Keywords

fly ash, SO₂ absorption, reaction kinetics

Disciplines

Bioresource and Agricultural Engineering | Environmental Engineering | Environmental Sciences

Comments

This is a manuscript of an article published as Li, Ling, Maohong Fan, Robert C. Brown, Jacek A. Koziel, and J. van Leeuwen. "Kinetics of SO₂ Absorption with Fly Ash Slurry with Concomitant Production of a Useful Wastewater Coagulant." *Journal of Environmental Engineering* 136, no. 3 (2009): 308-315. DOI: [10.1061/\(ASCE\)EE.1943-7870.0000155](https://doi.org/10.1061/(ASCE)EE.1943-7870.0000155). Posted with permission.

The kinetics of SO₂ absorption with fly ash slurry with concomitant production of a useful wastewater coagulant

Ling Li^{*a}, Maohong Fan^b, Robert C. Brown^c, Jacek A. Koziel^{d,a}, J(Hans) van Leeuwen^{a,d,e}

^a Department of Civil and Environmental Engineering, Iowa State University, Ames, IA, 50011

^b School of Materials Science and Engineering, Georgia Institute of Technology, Atlanta, GA, 30332

^c Center for Sustainable Environmental Technologies, Iowa State University, Ames, IA, 50011

^d Department of Agricultural and Biosystems Engineering, Iowa State University, Ames, IA, 50011

^e Department of Food Science and Human Nutrition, Iowa State University, Ames, IA, 50011

* Corresponding author. Tel.:+1-515-281-8892, Email: liling99@gmail.com

Abstract

This research was aimed at recovering Fe and Al compounds to produce a useful complex coagulant from fly ash using H₂SO₄ and SO₂ from flue gas oxidized to SO₃ by NaClO₃. The reaction kinetics of wet SO₂ scrubbing from simulated flue gas with fly ash slurry was studied. The SO₂ scrubbing experiments were carried out in a jacketed glass reactor system with a simulated flue gas containing SO₂ and N₂ in the gas phase and fly ash slurry in the liquid phase. Sodium chlorate was added to oxidize SO₂ to SO₃, adding H₂SO₄ in the slurry. The reaction orders of both Fe₂O₃ and Al₂O₃ extraction from fly ash slurry were shown to be 1.5th. The empirical Arrhenius expressions were also derived from the reaction rate constants obtained at each reaction temperature. The mass transfer process of SO₂ with ClO₃⁻ was evaluated using a two-film theory model.

Key words: fly ash; SO₂ absorption; reaction kinetics

1. INTRODUCTION

The emission of SO₂ in flue gas from coal combustion is a worldwide problem (WHO Regional Office of Europe, 2000). The most harmful impact of SO₂ on the environment is acid rain, which causes acidification of water bodies, soils, corrosion of material surfaces, and reduced growth of plants. In addition, when present with humidity in the air, SO₂ increases secondary fine particulate pollutant levels and

reduces visibility (National Air Pollutant Control Administration, 1970). Wet and dry SO₂ scrubbing with calcium sorbents have been used as the main SO₂ removal technologies for decades. However, the primary disadvantage of this traditional technique is the disposal of large amounts of byproduct slurry and separation and/or dewatering costs on top. Therefore, any possible use for SO₂ would be very attractive. Recent studies in our research group show that SO₂ can be used as a raw material in producing polymeric ferric sulfate (PFS), an effective wastewater treatment coagulant, using inexpensive ferrous sulfate solution and sodium chlorate Fan et al., 2000; Butler et al., 2004).

Another important waste from coal combustion is fly ash, which is a fine particulate material rich in Si, Fe, and Al oxides. Other elements, like Ca, Mg, Na, K are also present in smaller amount. The total amount of aluminum and iron oxides in fly ash can be as high as 75% (American Coal Ash Association, 2003), making it possible to extract those compounds for the production of aluminum sulfate and ferric sulfate, which are important wastewater treatment coagulants. Most iron- and aluminum-based sulfates on the market are produced from their ores. However, decreasing supplies of the minerals increase the cost of producing iron- and aluminum-based sulfates from the ores.

We have demonstrated the possibility of producing a complex polymeric Fe-Al coagulant by absorption and oxidation of SO₂ in fly ash slurry. This is providing a significant advantage for SO₂ removal using a power plant waste material and producing a valuable byproduct. Fan et al. investigated the synthesis and properties of PFS with SO₂ and proved that PFS had advantages over either Al₂(SO₄)₃ or Fe₂(SO₄)₃ (Fan et al., 2002; 2003a; 2003b). In addition, PFS is less corrosive and leaves less iron residual in water compared to other traditional iron coagulants (Fan et al., 2002). Recent research in our group also demonstrated that the complex polymeric coagulant containing both polymeric aluminum sulfate (PAS) and polymeric ferric sulfate (PFS) performed better than conventional iron- and aluminum-based coagulants in removing

total suspended solids (TSS) and turbidity from waste water (Li et al., 2008). Considering the advantages and disadvantages of individual Fe- and Al-based coagulants, a complex coagulant composed of both iron and aluminum could provide an alternative solution to the coagulation of wastewater (Fan et al., 2003a). The previous research investigated the reaction kinetics between fly ash and sulfuric acid (Fan et al., 2003a), and this paper also evaluated mass transfer process of SO₂. Although fly ash containing suitable amounts of Fe and Al can be used as the raw material to produce Fe- and Al-based complex coagulant, it is important to consider the potential leaching problem. Some researchers observed trace elements leaching from fly ash, resulting in ground water and soil contamination (Mohapatra and Rao, 2001). Therefore, a case-by-case test of fly ash application is still necessary.

The performances of the produced complex coagulant in the removal of total suspended solids and turbidity have been evaluated in our previous research (Fan et al., 2000; 2002). However, in order to develop this technology into a commercial process, more research needs to be done, and reaction kinetics is one of the most important aspects. This paper focuses on investigating the reaction kinetics of Fe₂O₃ and Al₂O₃ in fly ash with H₂SO₄ for their reaction orders and Arrhenius expressions under different reaction conditions. The optimum conditions of producing the complex coagulant from fly ash with the absorption of SO₂ were determined based on the reaction kinetics.

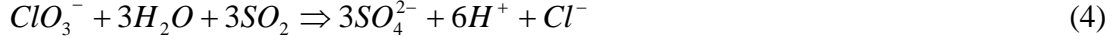
2. THE CHEMISTRY OF PRODUCING POLYMERIC COAGULANTS

The production of the complex polymeric iron-aluminum coagulant from fly ash with the absorption of SO₂ consists of the following steps.

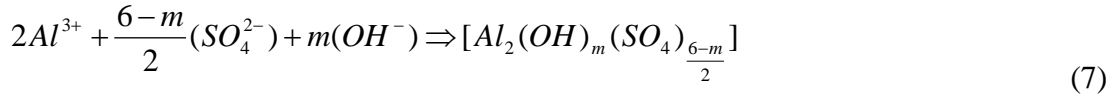
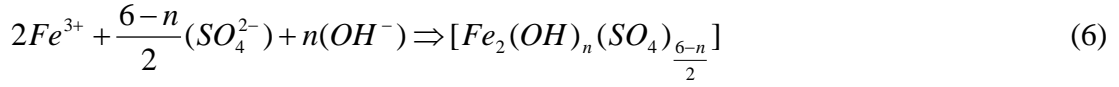
Fe₂O₃ and Al₂O₃ in fly ash react quickly with the added H₂SO₄ to produce Fe³⁺ and Al³⁺ (reaction 1 and 2).



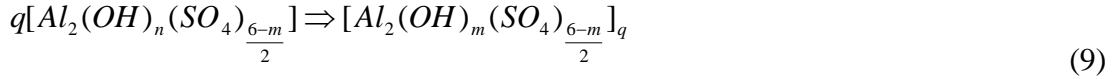
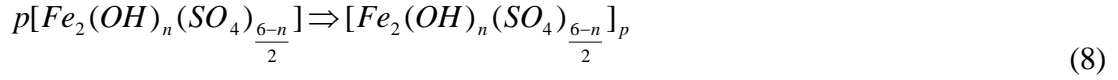
When SO_2 from the simulated flue gas dissolves in water, ClO_3^- in the fly ash slurry oxidizes SO_2 to SO_3 , resulting in additional SO_4^{2-} and H^+ (reactions 3 and 4),



Hydrolysis of iron and aluminum sulfates follows (reactions 5, 6 and 7)



Polymerization of ferric sulfate (PFS) and polymeric aluminum sulfate (PAS) follows (reactions 8 and 9) (Li et al, 2008).



The produced PFS and PAS based complex coagulate were successfully used in the removal of total suspended solids and turbidity in wastewater. This paper focuses on determining reaction kinetics in order to optimize the reaction conditions.

3. EXPERIMENTAL ASPECTS

3.1 Apparatus

The reaction of Fe_2O_3 and Al_2O_3 in fly ash with H_2SO_4 was conducted in a 500 ml jacketed glass reactor (ChemGlass Inc., Vineland, NJ, USA). The schematic of the reaction system used to determine reaction kinetics is shown in Fig. 1. There are five inlets on the reactor lid. A Teflon propeller was connected through the center inlet, stirring at 200 rpm. Prepared fly ash slurry was introduced into the reactor through the inlet with a funnel. A pump was connected to this inlet to dose oxidizer, i.e. $NaClO_3$ solution. After the fly ash slurry was added into the reaction, stirring with the

propeller was started, the funnel was removed and the inlet was sealed carefully with a glass stopper. A thermometer for temperature monitoring was connected to the third inlet. The fourth inlet was used to introduce the simulated flue gas, which contained N_2 and SO_2 , into the reactor. The fifth inlet was connected to a condenser, through which the outlet gas stream was released into the hood. The condenser was used to avoid water vapor escape in the outlet gas stream and return the condensate back to the reactor. A ZRF NDIR gas analyzer (Fuji Electric Co., Tokyo, Japan) was used to analyze SO_2 concentration in the outlet gas stream. A Dow Corning Fluid (Dow Chemical Co., Midland, MI, USA) was circulated through the reactor jacket by a Neslab RTE 111 heater unit.

3.2 Operation procedures

The fly ash sample was provided by HeadWaters Resource Inc. (South Jordan, UT, USA). The contents of Fe_2O_3 and Al_2O_3 in the fly ash were 25.48% and 21.03% respectively. In order to minimize the influence of soluble alkali, such as Na_2O and K_2O , the fly ash sample was washed with hot water and dried at 115 °C before being cooled down to room temperature. In each run, 100 g pretreated fly ash and 100 ml water were added into the reactor through a funnel. The fly ash slurry was stirred at 200 rpm at room temperature for about 1 hour to obtain a homogenous distribution. A heater unit was used to control the reaction temperature, which was monitored with a thermometer inserted into the reactor. When the desired temperature was reached, 50 mL 3.6 M H_2SO_4 was introduced into the reactor through a funnel and the simulated flue gas was bubbled through the stirred fly ash slurry at the same time. The flue gas was simulated by mixing 4% SO_2 and nitrogen to make a final concentration of SO_2 was controlled around 4000 ppm (by volume), which is at the high end of sulfur dioxide concentration in flue gas (Mayers et al., 2006). Sodium chlorate solution was made by adding 0.6 g was sodium chlorate into 50 mL distilled water and the solution was pumped into the reactor system in the first 10 minutes after the simulated flue gas was introduced, resulting in the oxidation of SO_2 . This experiment was run at seven

different temperatures, 70, 80, 90, 100, 110, 120, and 130 °C for 6 hours. The mixture was sampled with a 1 ml pipette every 30 min.

3.3 Determination of the concentrations of SO₂, iron and aluminum

The concentrations of SO₂ were analyzed with a ZRF NDIR gas analyzer, which was calibrated with a 0.5% SO₂ gas before each run. The concentrations of Al³⁺ in the produced coagulant were analyzed with an Agilent HP-4500 ICP-MS (Agilent Technologies, Santa Clara, CA, USA). The analysis of total Fe³⁺ in the produced coagulant was completed with a HACH 3000 (Hach Company, Loveland, CO, USA) spectrophotometer. All the samples were diluted properly according to the detection limits of the instrument prior to the analysis, and the instrument was calibrated with standard solutions at different concentrations before each run. A potassium permanganate titration method was used to determine ferrous iron concentration in the final product (Beijing University, 1993).

4. RESULTS AND DISCUSSION

4.1 Determination of reaction mechanism

Concentrations of Fe₂(SO₄)₃ and Al₂(SO₄)₃ in the produced complex coagulant are listed in Tables 1 and 2, The concentrations of Fe³⁺ increased with time and reaction temperature, and the concentration of Al³⁺ increased with time and reaction temperature until temperature reaches 120 °C. Since H₂SO₄ takes part in the conversion of Fe₂O₃ and Al₂O₃ in the fly ash, we derived the reaction kinetics based on the change of H₂SO₄ concentration. Let C_{s0} be the initial concentration of H₂SO₄, C_s be the concentration of H₂SO₄ in the reaction, and C_f and C_a be the concentration of Fe₂(SO₄)₃ and Al₂(SO₄)₃ respectively. According to the theory of multiple reactions, Eqs (1) and (2) can be considered as reversible parallel reactions (Walas, 1995; Levenspiel, 1999). Since Fe₂O₃ and Al₂O₃ are solids, the reaction rate of Fe₂(SO₄)₃ and Al₂(SO₄)₃ formation can be expressed as below.

$$\frac{dC_f}{dt} = k_1[C_s]^n \quad (10-a)$$

$$\frac{dC_a}{dt} = k_2 [C_s]^{n_2} \quad (11-a)$$

Because H₂SO₄ takes part in the reaction of both Fe₂O₃ and Al₂O₃ in the fly ash, the change of H₂SO₄ concentration is in proportion to the change of overall concentration of both Fe₂(SO₄)₃ and Al₂(SO₄)₃. Therefore, Eqs.(10-a) and (11-a) can be expressed as

$$\frac{dC_f}{dt} = k_1 [C_{s0} - 3(C_f + C_a)]^{n_1} \quad (10-b)$$

$$\frac{dC_a}{dt} = k_2 [C_{s0} - 3(C_f + C_a)]^{n_2} \quad (11-b)$$

After dividing Eq. (10) by Eq. (11), we get

$$\frac{dC_f}{dC_a} = \frac{k_1}{k_2} [C_{s0} - 3(C_f + C_a)]^{n_1 - n_2} \quad (12)$$

The ratio of Fe₂(SO₄)₃ and Al₂(SO₄)₃ concentrations was constant at each temperature, which indicates that the reaction orders , n_1 and n_2 are equal (Fan et al., 2003a). The statistical confidence level of this calculation is 95%, which indicates that there is a 95% certainty that the ratio of Fe₂(SO₄)₃ and Al₂(SO₄)₃ concentrations is constant at each temperature. The ratio of Fe₂(SO₄)₃ and Al₂(SO₄)₃ concentrations is presented in Fig. 2. Let n equal to n_1 and n_2 , then Eqs. (10) and (11) can be presented as:

$$\frac{dC_f}{dt} = k_1 [C_{s0} - 3(C_f + C_a)]^n \quad (13)$$

$$\frac{dC_a}{dt} = k_2 [C_{s0} - 3(C_f + C_a)]^n \quad (14)$$

The sum of Eqs. (13) and (14) gives

$$\frac{d(C_f + C_a)}{dt} = (k_1 + k_2) [C_{s0} - 3(C_f + C_a)]^n \quad (15)$$

Since n_1 and n_2 are equal, Eq. (12) can be simplified to

$$\frac{dC_f}{dC_a} = \frac{k_1}{k_2} \quad (16)$$

Integration of Eq. (16) gives

$$C_f = \frac{k_1}{k_2} C_a + C_{t,0} \quad (17)$$

where $C_{t,0}$ is the constant at $t = 0$. Since when the reaction started, the concentrations of both $\text{Fe}_2(\text{SO}_4)_3$ and $\text{Al}_2(\text{SO}_4)_3$ are zero, $C_{t,0}$ must be zero. Therefore, the relationship of k_1 and k_2 can be derived from Eq. (17)

$$\frac{k_1}{k_2} = \frac{C_f}{C_a} \quad (18)$$

Integration of Eq. (15) results in

$$\frac{1}{[C_{s0} - 3(C_f + C_a)]^{n-1}} = 3(n-1)(k_1 + k_2)t + \frac{1}{C_{s0}^{n-1}} \quad (19)$$

The values of C_f and C_a measured in the experiments are listed in Tables 1 and 2, and C_{s0} is 3.6 M. The relationship between $1/[C_{s0} - 3(C_f + C_a)]^{0.5}$ and t is plotted in Fig. 3, where C_{s0} is 3.6 M, and the linear relationship indicates that the value of $n-1$ is 0.5. Therefore, the value of n is 1.5, in other words, the reaction order of reaction (13) or (14) is 1.5. Therefore, Eq. (19) can be simplified to

$$\frac{1}{[C_{s0} - 3(C_f + C_a)]^{0.5}} = 1.5(k_1 + k_2)t + \frac{1}{C_{s0}^{0.5}} \quad (20)$$

The slope can be used to calculate k_1 and k_2 from Eq. (20):

$$k_1 + k_2 = \frac{1}{1.5} \text{slope} \quad (21)$$

The simultaneous solution of Eqs. (18) and (21) provides the reaction constants, k_1 and k_2 . The values of k_1 and k_2 are listed in Table 3.

4.2 Determination of Arrhenius expressions

The Arrhenius expression has been used to present the relationship between reaction rate constant and reaction temperature, as shown in Eq. (22).

$$k(T) = A \exp\left(\frac{-E}{RT}\right) \quad (22)$$

where A is frequency factor, E is activation energy (J/mole), T is absolute temperature (K) and R is gas constant (8.314 J/mole•K). Since this experiment was conducted in a

relatively narrow temperature range (70-130 °C), the variation of frequency factor and activation energy can be neglected (Fan et al., 2003a; Walas, 1995). The values of A and E for reaction (1) and (2) can be determined by the plotting $-\ln(k)$ vs. $1/T$, which indicates a linear relationship between $-\ln(k)$ and $1/T$, with correlation coefficient higher than 95%, as shown in Fig. 4. The relationship of the measured reaction rate constant and temperature can then be presented as below:

$$k_1(T) = 843.027 \exp\left(\frac{-4.852 \times 10^4}{RT}\right) \quad (23)$$

$$k_2(T) = 26.923 \exp\left(\frac{-3.641 \times 10^4}{RT}\right) \quad (24)$$

These results show that the activation energy of reaction (1) is greater than that of reaction (2), indicating that the reaction of Al_2O_3 is more sensitive to the reaction temperature.

4.2 Mass transfer evaluation of SO_2 absorption

The kinetics of SO_2 absorption in wet limestone scrubbing has been studied since wet limestone scrubbing became a commercial flue gas desulfurization process in the 1970s. However, there are still some problems regarding SO_2 modeling, particularly the SO_2 absorption (Olausson et al., 1993), which depends on reaction conditions. Therefore, a number of preliminary experiments were run in order to evaluate the physical characteristics of the gas-liquid mass transfer coefficients. The product of mass transfer coefficient and specific surface area ($k_g a$) of gas phase was evaluated by purging SO_2 containing gas into 0.1M NaOH solution, since SO_2 can be considered to be depleted completely at such a high pH value and therefore the mass transfer of liquid phase can be neglected. The product of mass transfer coefficient and specific surface area ($k_L a$) of liquid phase was evaluated by using 0.1M HCl solution to absorb SO_2 , where only physical absorption is considered (Lancia et al., 1997). However, both liquid phase and gas phase resistance have to be considered in the evaluation of

liquid-side mass transfer coefficient, which was calculated based on the overall mass transfer coefficient and gas side mass transfer coefficient.

The physical properties of SO₂ absorption and diffusivity are listed in Table 4 and the experimental results for SO₂ absorption are summarized in Table 5.

The absorption of SO₂ involves two steps, as shown in Eqs. (3) and (4). The reaction between dissolved SO₂ and sodium chlorate is instantaneous and irreversible; therefore, most of the dissolved SO₂ is consumed by reaction (4) and the reaction occurs at the gas-liquid interface. Assume each gas bubble follows a plug-flow pattern in the reactor, the driving force for SO₂ absorption can be considered as the difference of the average pressure of SO₂ in bulk flow and the partial pressure of SO₂ in equilibrium with liquid phase, defined as Δp_{SO_2} , as shown in Eq. (25). The average pressure of SO₂ in bulk flow can be evaluated by taking the logarithmic average of the inlet and outlet pressure (Lancia et al., 1997).

$$\Delta p_{SO_2} = p_{SO_2} \Big|_{ave} - H_{SO_2} C_{SO_2(aq)} \quad (25)$$

A diffuser was used to improve SO₂ removal efficiency. Based on the data in Tables 4 and 5, the enhancement factor of SO₂ mass transfer and overall mass transfer coefficient can be estimated. Since the reaction of SO₂ with ClO₃⁻ is instantaneous and irreversible, the enhancement factor for infinitely fast reaction Φ_a can be calculated using Eq. (26) (Levenspiel, 1996).

$$\phi_a = 1 + \frac{C_{ClO_3^-,0}}{nC_{SO_2,0}} \left(\frac{D_{ClO_3^-}}{D_{SO_2}} \right)^{0.5} \quad (26)$$

where n is 1/3, the molar ratio of ClO₃⁻ to SO₂ in reaction (4), $C_{ClO_3^-,0}$ is the initial concentration of ClO₃⁻, $C_{SO_2,0}$ is the initial aqueous concentration of SO₂, $D_{ClO_3^-}$ and D_{SO_2} are the diffusivity coefficients of ClO₃⁻ and SO₂ respectively. With the value of Φ_a , the liquid film enhancement factor Φ can be evaluated using a graph method

(Levenspiel, 1996). The overall mass transfer coefficient can be evaluated by Eq. (27).

$$\frac{1}{K_G} = \frac{1}{k_g a} + \frac{1}{k_L a H \phi} \quad (27)$$

The results of mass transfer coefficient for SO₂ absorption with/without diffuser are summarized in Table 6.

It was observed from Table 6 that when a diffuser was used, the mass transfer resistance in the gas phase was reduced greatly. It was also observed from Table 6 that over 95% overall mass transfer resistance is from the gas phase, which indicates that the mass transfer of SO₂ into the slurry is gas-film controlled. The total mass transfer resistance for both phases was also reduced in the experimental temperature range. The results indicate that the reaction of SO₂ with ClO₃⁻ is mass transfer controlled.

In a reaction system where mass transfer also takes place, a dimensionless number, the Damköhler number is usually used to determine the effect of mass transfer on the chemical reaction. Damköhler number is defined as the ratio of the chemical reaction rate to the mass transfer rate (Inglezakis and Pouloupoulos, 2006). The chemical reaction rate of SO₂ with ClO₃⁻ can be presented as

$$r_{SO_2} = k C_{SO_2} \quad (28)$$

where k is the SO₂ reaction rate constant described in Table 4 and C_{SO₂} is the concentration of SO₂ in liquid phase. In the reaction of SO₂ with ClO₃⁻, mass transfer is gas film controlled, therefore, the mass transfer rate can be presented as

$$N_A = K_G \Delta p_{SO_2} \quad (29)$$

where N_A is the mass transfer rate, K_G is the overall mass transfer coefficient calculated in Table 6 and Δp_{SO₂} is the driving force of SO₂ absorption as defined in Eq.(25).

Damköhler number can then be determined by the following equation

$$D_a = \frac{kC_{SO_2,0}^2}{K_G \Delta p_{SO_2}} \quad (30)$$

Damköhler number at different temperatures is listed in Table 7.

It was observed from Table 7 that the Damköhler number at each reaction temperature for both diffusing methods is at least in the order of 10^4 , which indicates that the global rate of SO_2 absorption is dominated by mass transfer (Inglezakis and Pouloupoulos, 2006). The Damköhler number with diffuser is higher than that without diffuser at each temperature. It was also noted that using a diffuser increased the overall mass transfer coefficient in Table 6. Therefore, a diffuser in the reaction system cannot only enhance mass transfer procedure of SO_2 absorption, but also increase the reaction rate. The ratio of D_a with diffuser to D_a without diffuser indicates that the absorption procedure of SO_2 with ClO_3^- is not favored by higher temperatures.

Since the reaction of SO_2 with ClO_3^- can be considered as an instantaneous irreversible reaction, the SO_2 diffusion in a homogeneous chemical reaction system, mass balance on SO_2 over a thickness Δx of the aqueous phase can be expressed in Eq. (28). The mass transfer model of SO_2 and ClO_3^- in a single gas bubble is shown in Fig. 5 and can be described as follows:

$$\frac{dN_{SO_2x}}{dx} + k' C_{SO_2} = 0 \quad (31)$$

where N_{SO_2} represents the molar flux of SO_2 at the position of x . Assume the dissolved SO_2 undergoes a first order reaction with ClO_3^- , and k' is the reaction rate for the reaction of SO_2 with ClO_3^- . Since the SO_2 concentration is low in the liquid phase, the flux of SO_2 can be written as below (Bird et al., 2002)

$$N_{SO_2x} = -D \frac{dC_{SO_2}}{dx} \quad (32)$$

where D is the diffusion coefficient of SO_2 in liquid phase.

The absorption of SO_2 with ClO_3^- could be expressed by substituting Eq. (31) into Eq. (32), leading to the following differential equation

$$D \frac{d^2 C_{\text{SO}_2}}{dx^2} - k' C_{\text{SO}_2} = 0 \quad (33)$$

When a stirrer and the diffuser are applied in the system, the gas-absorption process could be semi-quantified with the following reasonable assumptions. Gas bubbles are evenly distributed into the system, and each gas bubble is surrounded by a stagnant liquid film, as depicted in Fig. 5. A semi-steady concentration profile in the liquid film is quickly established after the gas bubbles are formed. The concentration of SO_2 outside the stagnant liquid film changes slowly and is considered constant, $C_{\text{SO}_2, \sigma}$.

Based on the assumptions mentioned above, the boundary conditions can be described below

$$\text{B.C.1: at } x=0, C_{\text{SO}_2}=C_{\text{SO}_2,0} \quad (34\text{-a})$$

$$\text{B.C.2: at } x=\sigma, C_{\text{SO}_2}=C_{\text{SO}_2, \sigma} \quad (34\text{-b})$$

With these boundary conditions, Eq. (33) can be solved:

$$\frac{C_{\text{SO}_2}}{C_{\text{SO}_2,0}} = \frac{\sinh \alpha \cosh \alpha \beta + (A - \cosh \alpha) \sinh \alpha \beta}{\sinh \alpha} \quad (35)$$

where α is a dimensionless group $\sqrt{k' \sigma^2 / D}$, and β is a dimensionless length, x/σ . A is $C_{\text{SO}_2, \sigma} / C_{\text{SO}_2,0}$, a constant which can be solved by analyzing the mass balance at $x=\sigma$.

Since the concentration of SO_2 , $C_{\text{SO}_2, \sigma}$ is considered at constant, the amount of SO_2 entering the bulk liquid at $x=\sigma$ over the entire bubble surface is equal to the amount of SO_2 consumed in the bulk liquid.

$$-SD \left. \frac{dC_{\text{SO}_2}}{dx} \right|_{x=\sigma} = V k' C_{\text{SO}_2, \sigma} \quad (36)$$

where V is the total volume of liquid phase. Therefore, the constant A in Eq. (35) can be solved by substituting Eq. (36) into Eq. (35).

$$A = \frac{1}{\cosh \alpha + (V/S\sigma)\alpha \sinh \alpha} \quad (37)$$

Since the value of α is very large, A is very nearly zero. Therefore, Eq. (35) can be simplified to

$$\frac{C_{SO_2}}{C_{SO_2,0}} = \frac{\sinh \alpha \cosh \alpha \beta - \cosh \alpha \sinh \alpha \beta}{\cosh \alpha} \quad (38)$$

For large values of α , $C_{SO_2}/C_{SO_2,0}$ increases with σ , which indicates that the amount of SO_2 reacts with ClO_3^- in the liquid film increases. Therefore, the untreated SO_2 in gas phase decreases, resulting in an improvement in SO_2 removal efficiency. The experimental results of SO_2 absorption showed that the stirrer and diffuser helped in improving SO_2 removal efficiency, indicating that the system is mass transfer controlled. This result also indicates that lower initial SO_2 concentration will result in higher removal efficiency.

5. CONCLUSIONS

The reaction kinetics for Fe_2O_3 and Al_2O_3 in fly ash under different reaction conditions including reaction temperatures, reaction time, and particle size was successfully derived. The model established shows that Fe_2O_3 and Al_2O_3 have the same reaction orders at the same reaction temperature. The reaction order of Fe_2O_3 or Al_2O_3 is 1.5. At the same reaction temperature, the reaction rate constant for Fe_2O_3 is higher than that of Al_2O_3 , and the activation energy in Arrhenius expression for Fe_2O_3 is greater than that of the reaction of Al_2O_3 . Therefore, reaction temperature has a larger impact on the extraction of Al_2O_3 from fly ash than that of Fe_2O_3 .

The mass transfer coefficient of SO_2 absorption and dimensionless number D_a describing the ratio of the chemical reaction rate to the mass transfer rate were evaluated. The results show that the absorption procedure of SO_2 with the reaction

system is mass transfer controlled. Semi-quantification of SO₂ absorption indicates that proper stirring and diffusing of the gas bubbles can enhance SO₂ mass transfer.

This research provides a possible utilization of fly ash in the production of an effective complex coagulant with the removal of SO₂ in flue gas. However, there are still some possible concerns of this procedure. Although over 70% of Fe₂O₃ and 40% of Al₂O₃ can be extracted from the fly ash, the inactive silicate and aluminosilicate still amount over 50%. However, the silicate and aluminosilicate materials could react with calcium hydroxide at to produce cementitious compounds in the presence of water if the physical and chemical properties meet the requirement. Therefore, future research on utilizing the inactive silicate and aluminosilicate slurry is necessary. Sodium chlorate was added as the oxidant in this study. Although sodium chlorate is effective in oxidizing SO₂, it is a non-selective herbicide. If residual sodium chlorate is discharged into the environment, it may impose harmful impacts on various plants. Therefore, a strict control of sodium chlorate discharge or finding an alternative oxidant is also important.

6. ACKNOWLEDGEMENT

We appreciate the assistance of Mr. Benjamin Franklin in HeadWaters Resource Inc. in supplying the fly ash samples. We thank Dr. Warren E. Straszheim and Dr. Basudeb Saha at Iowa State University in the analysis of the fly ash samples and aluminum concentrations. We also thank USEPA and the Center for Sustainable and Environmental Technology (CSET) at Iowa State University for their financial support.

List of Terms

α	dimensionless group
β	dimensionless group
Φ	enhancement factor, dimensionless
C_f	concentration of Fe ₂ (SO ₄) ₃ , mol/L
C_a	concentration of Al ₂ (SO ₄) ₃ , mol/L
$C_{ClO_3,0}$	initial concentration of ClO ₃ ⁻ , mol/L
C_s	concentration of H ₂ SO ₄ , mol/L

$C_{s,0}$	initial concentration of H ₂ SO ₄ , mol/L
$C_{SO_2(aq)}$	aqueous SO ₂ concentration, mol/L
$C_{SO_2,0}$	initial concentration of aqueous SO ₂ , mol/L
D	diffusion coefficient,
$D_{ClO_3^-}$	diffusivity coefficient of ClO ₃ ⁻ , m ² /s
D_{SO_2}	diffusivity coefficient of SO ₂ , m ² /s
H_{SO_2}	Henry's constant for SO ₂ , mol/L·atm
k_1, k_2	reaction rate constants, units depending on the reaction order
k'	reaction rate for the reaction of SO ₂ with ClO ₃ ⁻
K_G	overall mass transfer coefficient, mole/L·s·atm
k_{ga}	gas phase mass transfer coefficient, mole/L·s·atm
k_{la}	liquid phase mass transfer coefficient, s ⁻¹
n in Eq.26	molar ratio of ClO ₃ ⁻ concentration and SO ₂ aqueous concentration
n in Eq.10-Eq.19	reaction order
N_A	mass transfer rate, mole/m ³ ·s
R	gas constant, 8.314 J/mole·K
r_{SO_2}	SO ₂ reaction rate, mole/m ³ ·s
S	surface area of all the bubbles, m ³
T	absolute temperature, K
V	total volume of liquid phase, m ³
Δp_{SO_2}	driving force for SO ₂ absorption, atm

REFERENCES

- American Coal Ash Association (ACAA) (2003). "Fly ash facts for highway engineers."
- Atkinson, R., Baulch, D.L., Cox, R.A., Crowley, J.N., Hampson, R.F., Hynes, R.G., Jenkin, M.E., Rossi, M.J., Troe, J. (2004). "Evaluated kinetic and photochemical data for atmospheric chemistry: Volume I - gas phase reactions of O_x, HO_x, NO_x and SO_x species." *Atmos. Chem. Phys.*, 4, 1461 – 1738.
- Beijing University (1993). Beijing University's Analytical Chemistry Experimental Manual, 182-185.
- Bird, R. B., Stewart, W. E., Lightfoot, E. N. (2002). "Transport Phenomena, 2nd Edition". John Wiley & Sons, Inc., New York.
- Butler, A.D., Fan, M., Brown, R.C., Cooper, A.T., van Leeuwen, J.(H)., Sung, S. (2004). "Absorption of dilute SO₂ gas stream with conversion to polymeric ferric

- sulfate for use in water treatment." *Chem. Eng. J.*, 98, 265-273.
- Byrne, P. Ph.D. (2001). "Mathematical modeling and experimental simulation of chlorate and chlor-alkali cells." Dissertation, Royal Institute of Technology (KTH), Stockholm, Sweden.
- Chen, C., Zeng, M., Liu, G., Chai, C., Yao, Y., Liu, B. (1993). "Chemical Engineering Principles".
- Fan, M., Brown, R.C., Sung, S.W., Zhuang, Y. A. (2000). "Process for synthesizing polymeric ferric sulfate using sulfur dioxide from coal combustion." *Annual International Pittsburgh Coal Conference 17th*, Pittsburgh, PA, 2222-2229.
- Fan, M., Brown, R.C., van Leeuwen, J.(H)., Nomura, M., Zhuang, Y. (2003a). "The kinetics of producing sulfate based complex coagulant from fly ash." *Chem. Eng. Process.*, 42, 1019-1025.
- Fan, M., Brown, R.C., Zhuang, Y., Cooper, A.T., Nomura, M. (2003b). "Reaction kinetics for a novel flue gas cleaning technology." *Environ. Sci. Technol.*, 37, 1404-1407.
- Fan, M., Sung, S., Brown, R.C., Wheelock, T.D., Laabs, F.C. (2002). "Synthesis, characterization, and coagulation of polymeric ferric sulfate." *J. Environ. Eng.*, 483-490.
- Inglezakis, V., Pouloupoulos, S. (2006). "Adsorption, Ion Exchange and Catalysis: Design of Operations and Environmental Applications, 1st Edition." Elsevier Science & Technology Books.
- Lancia, A., Musmarra, D., Pepe, F. (1997). "Modeling of SO₂ absorption into limestone suspensions." *Ind. Eng. Chem. Res.*, 36, 197-293.
- Levenspiel, O. O. (1996). "The Chemical Reaction Omnibook." Oregon State University Bookstores, Corvallis, Oregon.
- Levenspiel, O.O. (1999). "Chemical Reaction Engineering, 3rd Edition." John Wiley & Sons, Inc., New York.

Li, L., Fan, M., Brown, R.C., Koziel, J.A., van Leeuwen, J.(H). (2009). "Production of a new wastewater treatment coagulant from fly ash with concomitant flue gas scrubbing." *J. Hazard. Mat.*, 162, 1430-1437.

Mohapatra, R., Rao, J.R. (2001). "Review: Some aspects of characterization, utilization, and environmental effects of fly ash." *J. Chem. Technol. Biotechnol.*, 76, 9-26.

Myers, R.D., Ghosh, M., MacLeod, J. B., Bridle, M. K. (2006). "Integrated water treatment and flue gas desulfurization process." United States Patent 7037434.

National Air Pollution Control Administration. (1970). "Air quality criteria for sulfur oxides." Washington D.C.

Olausson, S., Wallin, M., Bjerle, I. (1993). "A model for the absorption of sulphur dioxide into a limestone slurry." *Chem. Eng. J.*, 51, 99-108.

Walas, S.M. (1995). "Chemical Reaction Engineering Handbook of Solved Problems." Gordon and Breach Publishers, Amsterdam.

WHO Regional Office of Europe, Air Quality Guidelines. (2000).